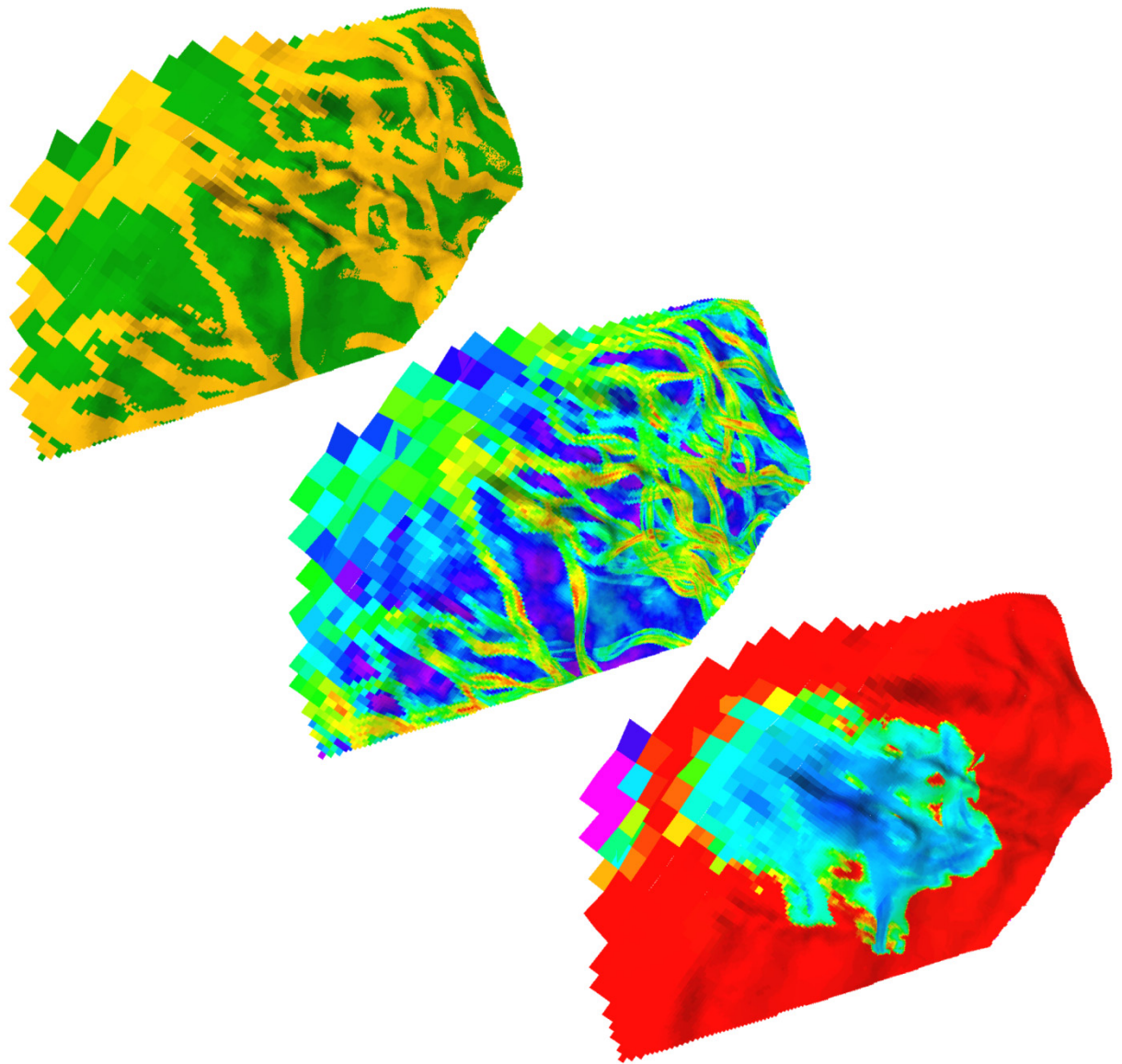


Managing the Interdisciplinary Requirements of 3D Geological Models



Sarah Jane Riordan
Australian School of Petroleum
University of Adelaide
March 2009

Thesis submitted in accordance with the requirements of the University of Adelaide
for the degree of Doctor in Philosophy

Abstract

Despite increasing computer power, the requirement to upscale 3D geological models for dynamic reservoir simulation purposes is likely to remain in many commercial environments. This study established that there is a relationship between sandbody size, cell size and changes to predictions of reservoir production as grids are upscaled. The concept of a cell width to sandbody width ratio (*CSWR*) was developed to allow the comparison of changes in reservoir performance as grids are upscaled.

A case study of the Flounder Field in the Gippsland Basin resulted in the interpretation of three depositional environments in the intra-Latrobe reservoir interval. The sandbody dimensions associated with these depositional environments were used to build a series of 3D geological models. These were upscaled vertically and horizontally to numerous grid cell sizes. Results from over 1400 dynamic models indicate that if the *CSWR* is kept below 0.3 there will be a strong correlation between the average production from the upscaled grids compared to those of a much finer grid, and there will be less than 10% variation in average total field production. If the *CSWR* is between 0.3 and 1, there could be up to 30% difference, and once the *CSWR* exceeds 1.0 there is only a weak relationship between the results from upscaled grids and those of finer grids.

As grids are upscaled the morphology of bodies in facies models changes, the distribution of petrophysical properties is attenuated and the structure is smoothed. All these factors result in a simplification of the fluid flow pathways through a model. Significant loss of morphology occurs when cells are upscaled to more than a half the width of the reservoir body being modelled. A simple rule of thumb is established — if the geological features of a model cannot be recognised when looking at a layer in the upscaled grid, the properties of the upscaled grid are unlikely to be similar to those of the original grid and the predictions of dynamic models may vary significantly from those of a finer grid.

This understanding of the influence of sandbody size on the behaviour of upscaled dynamic models can be used in the planning stages of a reservoir modelling project. Two simple charts have been created. The first chart is for calculating the approximate number of cells in a model before it is built. The second chart is for comparing the proposed cell size against the *CWSR*, so that the predicted discrepancy between the ultimate production from the upscaled grid and one with much smaller cells can be assessed. These two charts enhance discussion between all interested disciplines regarding the potential dimensions of both static and upscaled dynamic models during the planning stage of a modelling project, and how that may influence the results of dynamic modelling.

Thesis Declaration

This work contains no material which has been accepted for the award of any other degree or diploma in any university or other tertiary institution and, to the best of my knowledge and belief, contains no material previously published or written by another person, except where due reference has been made in the text.

I give consent to this copy of my thesis, when deposited in the University Library, being made available for loan and photocopying, subject to the provisions of the Copyright Act 1968.

Acknowledgements

Over the eight years that this thesis has taken I have worked my way through a number of excellent supervisors. I am indebted to Simon Lang and Tobi Payenberg for enthusiastically guiding me through the intricacies of interpreting the Flounder Field, to Jochen Kassin for his willingness to be on call for random modelling questions and to Bruce Ainsworth, who inherited me from Tobi towards the end, and gave me the benefit of his experience in model building and has helped me bring it all together.

The field data used in this project was supplied by ExxonMobil. Thanks to Mike Hordern at ExxonMobil for his advice and support.

All the staff at the ASP are wonderful, but special thanks must go to the endlessly patient Ian West for never telling me that my computer problems were caused by a squishware failure.

This thesis was completed in spite of the many (mainly) wonderful distractions provided by my daughters Alexandra and Vivian who entered my life along the way. I will always be grateful to my parents who provided me with the excellent emotional, educational, and financial foundations which have got me to this point in my life. The only way I can think of to repay such a gift, is to do my best to follow their example, and provide Alexandra and Vivian with the same sort of encouragement and opportunities that they gave to me.

The biggest thanks of all must go to my partner Terry who has kept me well supplied with computers, geeky gadgets, and diamonds throughout this process. This thesis would never have been started, let alone completed, without his continuous love, encouragement, technical support, and occasional boot up the backside.

For Mum - another milestone in my life you would have loved to see

Table of Contents

ABSTRACT	I
THESIS DECLARATION	III
ACKNOWLEDGEMENTS.....	V
TABLE OF CONTENTS	VII
TABLE OF FIGURES	IX
TABLE OF TABLES.....	XV
1 INTRODUCTION	1
1.1 STUDY RATIONALE	1
1.2 STUDY WORKFLOW	3
1.3 THESIS LAYOUT	5
2 CASE STUDY: FLOUNDER FIELD.....	9
2.1 INTRODUCTION.....	9
2.2 HISTORY.....	9
2.3 METHODOLOGY.....	13
2.4 DATA USED.....	13
2.5 INTERPRETATION.....	17
2.6 STRATIGRAPHIC INTERPRETATION.....	20
2.7 CORE INTERPRETATION – THIS STUDY.....	21
2.8 PALAEOGEOGRAPHY	30
2.9 SEQUENCE STRATIGRAPHY	35
2.10 FIGURES – FLOUNDER FIELD	39
3 DEPOSITIONAL ANALOGUES.....	91
3.1 INTRODUCTION.....	91
3.2 STRANDPLAIN SYSTEMS	92
3.3 BARRIER-ISLAND SYSTEMS	96
3.4 INCISED VALLEY FILL.....	104
3.5 POROSITY AND PERMEABILITY DISTRIBUTION	108
3.6 FLOW UNIT BOUNDARIES	112
3.7 DISCUSSION – DEPOSITIONAL ENVIRONMENTS	114
3.8 CONCLUSIONS – DEPOSITIONAL ANALOGUES.....	117
3.9 FIGURES – DEPOSITIONAL ANALOGUES	119
4 STATIC MODELS.....	157
4.2 INTRODUCTION.....	157
4.3 METHODOLOGY.....	159
4.4 FACIES MODELS.....	160
4.5 PETROPHYSICAL MODELS	165
4.6 DISCUSSION – STATIC MODELS.....	167
4.7 FIGURES – STATIC MODELS.....	169

5	UPSCALING.....	181
5.1	METHODOLOGY	181
5.2	RESULTS OF UPSCALING THE MODELS	182
5.3	DISCUSSION – UPSCALING.....	188
5.4	CONCLUSIONS – UPSCALING	191
5.5	FIGURES – UPSCALING	193
6	DYNAMIC MODELS.....	241
6.1	INTRODUCTION	241
6.2	METHODOLOGY	242
6.3	RESULTS.....	246
6.4	DISCUSSION – DYNAMIC MODELS.....	257
6.5	CONCLUSIONS – DYNAMIC MODELLING	261
6.6	FIGURES & TABLES– DYNAMIC MODELLING.....	263
7	FROM GEOLOGICAL INTERPRETATION TO DYNAMIC MODEL	339
7.1	INCORPORATING ANALOGUES INTO THE MODEL DESIGN PROCESS	339
7.2	STATIC PARAMETERS, UPSCALING AND SIMULATION	340
7.3	SCOPE FOR FURTHER WORK	345
7.4	THE WAY FORWARD – HOW DO THE RESULTS APPLY TO FUTURE MODELLING	347
7.5	FIGURES & TABLES– GEOLOGICAL INTERPRETATION TO DYNAMIC MODELS.....	351
8	CONCLUSIONS	365
8.1	FLOUNDER FIELD STUDY	365
8.2	ANALOGUE DATA	365
8.3	3D MODELLING	366
9	REFERENCES.....	371
APPENDIX 1.	CORE LOGS	393
APPENDIX 2.	LOG SIGNATURE & PALAEOFACIES MAPS.....	401
APPENDIX 3.	POROSITY UPSCALING	421
APPENDIX 4.	PORE VOLUMES.....	431
APPENDIX 5.	DYNAMIC MODEL UPSCALING.....	437

Table of Figures

FIGURE 1.1. WORKFLOW FOLLOWED IN THIS THESIS.	7
FIGURE 1.2. GRID DESIGN AND UPSCALING.	8
FIGURE 2.1. GIPPSLAND BASIN, STRUCTURAL SETTING.....	41
FIGURE 2.2. STRATIGRAPHIC UNITS AND UNCONFORMITIES WITHIN THE GIPPSLAND BASIN.	42
FIGURE 2.4. SEISMIC INLINE, SHOWING THE TOP OF THE LATROBE GROUP, THE TUNA–FLOUNDER CHANNEL AND THE FAULTED INTRA-LATROBE GROUP.	44
FIGURE 2.5. TYPE LOG FOR THE FLOUNDER FIELD—FLOUNDER 6ST1 SHOWING PREVIOUS INTERPRETATIONS OF THE ZONE OF INTEREST.....	45
FIGURE 2.6. WIRELINE LOGS AVAILABLE IN EACH WELL IN THE FLOUNDER FIELD DATASET.	46
FIGURE 2.7. FLOUNDER FIELD CORES STUDIED.	47
FIGURE 2.8. SURFACES INTERPRETED IN THE UPPER ROUNDHEAD MEMBER TO UPPER VOLADOR FORMATION INTERVAL.	48
FIGURE 2.9. FLOUNDER 6 STRATIGRAPHY AND GLOBAL SEA-LEVEL CURVES.	49
FIGURE 2.11. CORE LOG, FLOUNDER 6 ST1 SHOWING KEY SEDIMENTARY STRUCTURES AND THE FACIES ASSOCIATIONS.	51
FIGURE 2.12. FLOUNDER 6 ST1 CORE 10, UPPER VOLADOR FORMATION, FACIES ASSOCIATION 1, SHOWING FLASER BEDDING AND OYSTER SHELLS.	52
FIGURE 2.13. FLOUNDER 6ST1 CORE, VU.0 AND VU.1 UNITS. UPPER VOLADOR FORMATION, SHOWING DETAIL OF A WASHOVER FAN	53
FIGURE 2.14. FLOUNDER A4, UPPER ROUNDHEAD MEMBER RL.5 AND RL.6 UNITS.	54
FIGURE 2.15. FLOUNDER 6 ST1, CORE 9. VU.2 UNIT.	55
FIGURE 2.16. FLOUNDER 6 ST1, VU.3 & VU.4.....	56
FIGURE 2.17. FLOUNDER 6 ST1 CORE, VU.4 AND RL.1 UNITS.	57
FIGURE 2.18. FLOUNDER 6ST1, CORE 7, RL.1 TO RL.3 UNIT, FA 6.	58
FIGURE 2.19. FLOUNDER A4. FACIES ASSOCIATIONS 5 AND 7.	59
FIGURE 2.20. FLOUNDER A4. FACIES ASSOCIATION 7.	60
FIGURE 2.21. FLOUNDER 6 CORE 3, RL.7 AND RU.1 UNIT, SHOWING SB2.	61
FIGURE 2.22. UPPER ROUNDHEAD MEMBER CORES 1 AND 2, FLOUNDER 6.	62
FIGURE 2.23. FLOUNDER 3, CORE 2, RU.4 UNIT.....	63
FIGURE 2.24. FLOUNDER A2 CORES 2 & 3, RU.3 AND RU.4 UNITS.	64
FIGURE 2.25. FLOUNDER 6ST1 CORE 4, RU.4 UNIT, SHOWING A TRANSGRESSIVE LAG (FA11) AT THE TOP OF THE UPPER ROUNDHEAD MEMBER.	65
FIGURE 2.26. FLOUNDER A2, CORES 1 & 2, RU.4 UNIT.	66
FIGURE 2.27. IDEALISED SECTION OF AN INCISED VALLEY SYSTEM	67
FIGURE 2.29. UPPER VOLADOR FORMATION. PALAEOFACIES MAPS AND RELATIVE SEA LEVEL CURVE.	69
FIGURE 2.33. LOWER ROUNDHEAD MEMBER PALAEOFACIES MAPS AND RELATIVE SEA LEVEL CURVE.	73
FIGURE 2.34. LOG SIGNATURE PLOT AND PALAEOFACIES MAP OF THE RL.1 UNIT.....	74
FIGURE 2.36. LOG SIGNATURE PLOT AND PALAEOFACIES MAP OF THE RL.4 UNIT.	76
FIGURE 2.41. VARIANCE SLICE FROM THE NORTHERN FIELDS SURVEY.	81
FIGURE 2.43. UPPER ROUNDHEAD MEMBER PALAEOFACIES MAPS AND RELATIVE SEA LEVEL CURVE.	83
FIGURE 2.46. LOG SIGNATURE AND PALAEOFACIES MAP OF RU.3 UNIT.	86
FIGURE 3.1. SCHEMATIC SHOWING HOW THE WIDTH OF MODERN BARRIER ISLANDS OR STRANDPLAINS CAN BE USED AS AN ANALOGUE FOR THE MODELLING OF ANCIENT SYSTEMS.	121
FIGURE 3.2. SHOREFACE ELEMENTS.....	122
FIGURE 3.3. IDEALIZED VERTICAL SHOREFACE PROFILE.	123
FIGURE 3.4. SANDBODY TYPES AND THEIR AVERAGE DIMENSIONS IN DELTAIC SYSTEMS.	124
FIGURE 3.5. WIDTH VS. THICKNESS OF SHORELINE-SHELF SANDBODIES LESS THAN 50 KM WIDE.	125
FIGURE 3.6. THE INTERACTION BETWEEN LONGSHORE DRIFT, FLUVIAL DISCHARGE AND FLUVIAL SEDIMENT TYPE.	126
FIGURE 3.7. POTENTIAL MODERN ANALOGUES FOR THE LOWER ROUNDHEAD MEMBER.	127

FIGURE 3.8. MOUTH OF THE RIVER DOCE, BRAZIL.	128
FIGURE 3.9. BARRIER ISLAND FORMATION THROUGH SPIT DETACHMENT.	129
FIGURE 3.10. BARRIER ISLAND FORMATION THROUGH THE DROWNING OF BEACH RIDGES DURING RELATIVE SEA LEVEL RISE.	129
FIGURE 3.11. BARRIER ISLAND FORMATION VIA BAR EMERGENCE.	130
FIGURE 3.12. FORMATION OF TRANSGRESSIVE BARRIER ISLANDS ON THE MISSISSIPPI DELTA FRONT.	131
FIGURE 3.13. ELEMENTS OF A TRANSGRESSIVE BARRIER ISLAND SYSTEM.	132
FIGURE 3.14. PART OF THE GIPPSLAND LAKES BARRIER ISLAND SYSTEM, VICTORIA.	133
FIGURE 3.16. A COMPARISON OF THE DEPOSITS FOUND IN TIDE- AND WAVE-DOMINATED TIDAL INLETS.	135
FIGURE 3.17. MODIFIED LANDSAT IMAGE SHOWING TIDAL-DELTA COMPLEX, MORETON BAY, QUEENSLAND.	136
FIGURE 3.18. WASHOVERS ON DAUPHIN ISLAND, GULF OF MEXICO AFTER HURRICANE KATRINA.	137
FIGURE 3.19. LENGTH VS. WIDTH OF MODERN BARRIER ISLANDS, MEASURED OFF LANDSAT IMAGES.	138
FIGURE 3.20. CROSS SECTION THROUGH ROANOKE ISLAND AND OUTER BANKS, NORTH CAROLINA.	139
FIGURE 3.21. A COMPARISON OF THE WIDTHS OF MODERN AND ANCIENT BARRIER ISLANDS.	140
FIGURE 3.22. LENGTH VS. WIDTH OF FLOOD TIDAL DELTA COMPLEXES.	141
FIGURE 3.23. FREQUENCY PLOT OF TIDAL CHANNEL WIDTHS.	142
FIGURE 3.24. BLOCK DIAGRAMS SHOWING THE DIFFERENCES IN SEDIMENTATION PATTERNS BETWEEN HIGH SINUOSITY CHANNELS (A) AND LOW SINUOSITY CHANNELS (B).	143
FIGURE 3.25. YUKON RIVER, ALASKA.	144
FIGURE 3.26. DIFFERENT SCALES OF RIVER CHANNEL DEPOSITS.	145
FIGURE 3.27. A COMPARISON OF THE DEPOSITIONAL FACIES AND THEIR DISTRIBUTION BETWEEN A WAVE-DOMINATED DELTA (TOP) AND A TIDE-DOMINATED DELTA (BOTTOM).	146
FIGURE 3.28. CLASSIFICATION OF COASTAL ENVIRONMENTS.	147
FIGURE 3.29. ELEMENTS OF A WAVE-DOMINATED ESTUARY.	148
FIGURE 3.30. CHANGES IN DEPOSITIONAL FACIES DISTRIBUTION AS A WAVE-DOMINATED ESTUARY IS FILLED.	149
FIGURE 3.31. SUPERIMPOSED CHANNEL BARS AND CHANNEL BELTS WITHIN A SINGLE CHANNEL BELT COMPLEX.	150
FIGURE 3.32. CHANNEL DEPTH TO CHANNEL BELT WIDTH RATIOS, SHOWING UPPER ROUNDHEAD RU.1 UNIT DIMENSION.	151
FIGURE 3.34. FLUVIAL STACKING PATTERNS AND THEIR RELATIONSHIP TO SYSTEMS TRACTS.	153
FIGURE 3.35. A COMPARISON OF FLUVIAL AND SHOREFACE DEPOSITS.	154
FIGURE 4.1. BRIEF FLOW PATH OF MODELLING PROCESS FOR THIS STUDY.	171
FIGURE 4.2. RMS SCREEN CAPTURES SHOWING THE THREE GRID DESIGNS USED—SQUARE, SSA AND SDA.	172
FIGURE 4.3. CROSS SECTION SHOWING THE UPPER ROUNDHEAD MEMBER TO UPPER VOLADOR FORMATION INTERVAL.	173
FIGURE 4.4. BUILDING THE COASTAL FACIES MODEL.	174
FIGURE 4.5. FACIES MODEL OF UPPER VOLADOR FORMATION BARRIER ISLAND SYSTEM.	175
FIGURE 4.6. FLATTENED SECTION OF SHOREFACE FACIES MODEL.	176
FIGURE 4.7. POROSITY MODELS—INDIVIDUAL LAYERS.	177
FIGURE 4.8. POROSITY DISTRIBUTION HISTOGRAMS.	178
FIGURE 4.9. POROSITY DISTRIBUTION HISTOGRAMS OF RESERVOIR FACIES.	179
FIGURE 4.10. CROSS PLOT OF CORE POROSITY VS. CORE PERMEABILITY.	180
FIGURE 5.1. MATRICES SHOWING THE GRID DESIGNS BUILT AND HOW THEY WERE UPSCALED.	195
FIGURE 5.2. NUMBER OF ACTIVE CELLS IN THE MODELS BUILT.	196
FIGURE 5.3. VERTICAL UPSCALING OF CHANNELS.	197
FIGURE 5.4. SQ280-25 SCENARIO, 24 LAYERS.	198
FIGURE 5.5. VERTICAL AND HORIZONTAL UPSCALING OF SELECTED GRIDS. SQ280-25 SCENARIO.	199
FIGURE 5.6. SSA280-25 SCENARIO, 24 LAYERS.	200
FIGURE 5.7. SDA280-25 SCENARIO.	201
FIGURE 5.8. CONCEPTUAL COASTAL MODEL.	202
FIGURE 5.9. THE INFLUENCE OF GRID CELL SHAPE ON THE UPSCALING OF POROSITY MODELS.	203
FIGURE 5.10. THE RELATIONSHIP BETWEEN CELL WIDTH AND CHANNEL WIDTH.	204
FIGURE 5.11. HORIZONTAL UPSCALING OF BEACH MODEL—24-LAYER GRID.	205

FIGURE 5.12. VERTICAL UPSCALING OF THE COAST SCENARIO—SQUARE GRID.....	206
FIGURE 5.14. VERTICAL UPSCALING OF THE COAST SCENARIO—SSA GRID.....	208
FIGURE 5.15. POROSITY MODEL OF A CONCEPTUAL FLUVIAL CHANNEL MODEL.....	209
FIGURE 5.16. HISTOGRAM OF POROSITY VALUES FOR GRIDS SHOWN IN	210
FIGURE 5.17. CHANGING POROSITY DISTRIBUTION WITH VERTICAL UPSCALING—SQUARE GRID.	211
FIGURE 5.18. SILHOUETTES OF THE POROSITY DISTRIBUTIONS FOR ALL GRIDS. SQ100-25 SCENARIO.	212
FIGURE 5.19. HISTOGRAM OF POROSITY VALUES FOR THE 24 LAYER SDA100-50 SCENARIO.	213
FIGURE 5.20. A COMPARISON OF THE POROSITY DISTRIBUTION OF THE 25% AND 50% GROSS SAND, 100 M CHANNEL SCENARIOS (SQUARE GRID).....	214
FIGURE 5.21. POROSITY MODEL AND HISTOGRAM OF SQ280-25 SCENARIO, 24 LAYERS.	215
FIGURE 5.22. UPSCALING HIGH PERMEABILITY STREAKS IN 280 M WIDE CHANNELS—SQUARE GRID DESIGN.	216
FIGURE 5.23. VERTICAL UPSCALING OF POROSITY IN THE BEACH SCENARIO.....	217
FIGURE 5.24. POROSITY DISTRIBUTION FOR THE SQ BEACH SCENARIO, ALL LAYERS.	218
FIGURE 5.25. HISTOGRAMS OF POROSITY DISTRIBUTION IN THE SQ COAST SCENARIO.	219
FIGURE 5.26. POROSITY MODEL—SQ BEACH SCENARIO. 24 LAYERS.	220
FIGURE 5.27. POROSITY DISTRIBUTION OF THE SHOREFACE COMPONENT OF THE BEACH SCENARIO (SQUARE GRID).	221
FIGURE 5.28. A COMPARISON OF THE 'BEACH' AND 'COAST' POROSITY DISTRIBUTIONS—SQUARE GRID.....	222
FIGURE 5.30. BREAKDOWN OF POROSITY DISTRIBUTION FOR SQ COAST' SCENARIO BY FACIES. 1000 X 800 X 24 MODEL.	224
FIGURE 5.31. SQ COAST SCENARIO - SHOREFACE FACIES POROSITY DISTRIBUTION.	225
FIGURE 5.32. POROSITY DISTRIBUTION IN THE FLUVIAL FACIES IN THE SQ COAST SCENARIO.	226
FIGURE 5.33. PORE VOLUME BY FACIES (FL: FLUVIAL, OB: OVERBANK, TOT: TOTAL PORE VOLUME). 24 LAYERS, SQ 280-25 SCENARIO.	227
FIGURE 5.34. AVERAGE PORE VOLUME BY FACIES - BEACH SCENARIO.	228
FIGURE 5.35. MULTIPLE REALIZATIONS OF PORE VOLUME OF FACIES IN A COAST SCENARIO.	229
FIGURE 5.36. CHANGES TO THE AVERAGE PORE VOLUME OF THE FACIES IN THE COAST SCENARIO WITH VERTICAL UPSCALING.	230
FIGURE 5.37. THE IMPACT OF VERTICAL UPSCALING ON AVERAGE PORE VOLUME, SQ 100-25 SCENARIO.	231
FIGURE 5.38. CHANGE IN AVERAGE PORE VOLUME RELATIVE TO BASE MODEL. SQ 100-25 SCENARIO.	232
FIGURE 5.39. PORE VOLUME BY FACIES. 280-25 SCENARIO - ALL GRID DESIGNS. REALIZATIONS 1-3.	233
FIGURE 5.40. PORE VOLUME BY FACIES. 280-50 SCENARIO - ALL GRID DESIGNS. REALIZATIONS 1-3.	234
FIGURE 5.41. CHANGE IN FACIES PORE VOLUME RELATIVE TO BASE MODEL. SQUARE GRID, 24 LAYERS, ALL CHANNEL SCENARIOS.	235
FIGURE 5.42. VOLUME OF CHANNEL FACIES CONNECTED TO WELLS—SQ 280-25 SCENARIO.....	236
FIGURE 5.43. VOLUME OF FLUVIAL FACIES CONNECTED TO WELLS, SQ280-25 SCENARIO. REALIZATION 1.....	237
FIGURE 5.44. FLUVIAL FACIES CONNECTIVITY TO WELLS—3 LAYERS (EXCEPT FOR 1000 X 800 GRID WHICH IS 24 LAYERS).	238
FIGURE 5.45. THE IMPACT OF VERTICAL AVERAGING ON FACIES CONNECTIVITY BETWEEN A TIDAL CHANNEL AND UPPER SHOREFACE.	239
FIGURE 5.46. ALL CHANNEL BODIES IN THE SQ280-25 SCENARIO (REALIZATION 1).....	240
FIGURE 6.1. DEPTH STRUCTURES AND OIL WATER CONTACTS.	271
FIGURE 6.2. SUMMARY OF THE RESERVOIR SIMULATION CARRIED OUT FOR EACH GRID DESIGN.....	272
FIGURE 6.3. UPSCALING POROSITY AND CHANNEL FACIES.	273
FIGURE 6.4. SAMPLES OF WELL POSITION RELATIVE TO POROSITY.	274
FIGURE 6.5. ULTIMATE OIL PRODUCTION FOR THE HOMOGENEOUS MODEL—ALL GRID DESIGNS.	275
FIGURE 6.6. GRID DIMENSIONS AND NUMBER OF CELLS.	276
FIGURE 6.7. CELL DESIGN FOR THE SQUARE GRID, SHOWING LOCATION OF THE 5 VERTICAL WELLS (A,B,C,D,E).	277
FIGURE 6.8. CELL DESIGN FOR THE SDA GRID, SHOWING LOCATION OF THE 5 VERTICAL WELLS (A,B,C,D,E).....	278
FIGURE 6.9 CELL DESIGN FOR THE SSA GRID, SHOWING LOCATION OF THE 5 VERTICAL WELLS (A,B,C,D,E).....	279
FIGURE 6.10. WATER INFLUX INTO HOMOGENEOUS MODEL. 500 X 400 X 3 SQ GRID.	280
FIGURE 6.11. CUMULATIVE RECOVERY BY WELL. SQUARE GRID, HOMOGENEOUS MODEL.....	281
FIGURE 6.12. A COMPARISON OF THE ULTIMATE FIELD PRODUCTION OF THE 3-LAYER GRIDS WITH DIFFERENT GRID DESIGNS.....	282
FIGURE 6.13. SQUARE GRID HOMOGENOUS GRID. SIMULATION AT 20 YEARS, LAYER 3 OF MODEL (BASE).....	283

FIGURE 6.14. SDA GRID, HOMOGENEOUS MODEL. RESERVOIR SIMULATION RESULTS AT THE END OF 20 YEARS PRODUCTION, LAYER 3 OF MODEL (BASE).....	284
FIGURE 6.15. RESULTS OF RESERVOIR SIMULATION OF HOMOGENEOUS MODEL AT THE END OF 20 YEARS PRODUCTION.....	285
FIGURE 6.16. INDIVIDUAL WELL PRODUCTION FROM THE HOMOGENEOUS 3 LAYER SDA GRID.	286
FIGURE 6.17. INDIVIDUAL WELL PRODUCTION FROM THE HOMOGENEOUS 3 LAYER SSA GRID.....	287
FIGURE 6.18. A COMPARISON OF SIMULATION RESULTS FOR VERTICAL AND HORIZONTAL UPSCALING. 100-25 SCENARIO.	288
FIGURE 6.19. TOTAL FIELD PRODUCTION FOR THE 100-25 SCENARIO.	289
FIGURE 6.20. CHANGE IN ULTIMATE RECOVERY, SQ100-25 SCENARIO, 3 LAYERS.....	290
FIGURE 6.21. PRODUCTION CHARACTERISTICS OF REALIZATION 4 SQ100-25 SCENARIO.....	291
FIGURE 6.22. POROSITY DISTRIBUTION, SQ100-25 SCENARIO. REALIZATION 4.	292
FIGURE 6.23. CHANNEL PROXIMITY TO WELLS. REALIZATION 4, SQ100-25 SCENARIO.....	293
FIGURE 6.24. OIL SATURATION. WATER INJECTION PATTERNS AT THE END OF 20 YEARS. SQ100-25 SCENARIO, REALIZATION 4, LAYER 3 OF 3.	294
FIGURE 6.25. CUMULATIVE OIL AND WATER PRODUCTION FOR SQ100-25 SCENARIO, REALIZATION 5.	295
FIGURE 6.26. CHANNEL PROXIMITY TO WELLS. REALIZATION 5, SQ100-25 SCENARIO.....	296
FIGURE 6.27. OIL SATURATION. WATER INFLOW AT THE END OF 20 YEARS, SQ100-25 SCENARIO, REALIZATION 5, LAYER 3 OF 3.	297
FIGURE 6.28. REALIZATION 9, SQ100-25 SCENARIO.	298
FIGURE 6.29. CHANNEL PROXIMITY TO WELLS. REALIZATION 9, SQ100-25 SCENARIO.....	299
FIGURE 6.30. DETAIL OF POROSITY GRID AROUND WELL A, REALIZATION 9, SQ100-25 SCENARIO.....	300
FIGURE 6.31. RESERVOIR SIMULATION, WATER INFLUX. SQ100-25 SCENARIO, REALIZATION 9, LAYER 3 OF 3 AT 20 YEARS.....	301
FIGURE 6.32. PRODUCTION PROFILES OF REALIZATION 2. SQ100-25 SCENARIO.	302
FIGURE 6.33. CHANNEL PROXIMITY TO WELLS. REALIZATION 2, SQ100-25 SCENARIO.....	303
FIGURE 6.34. CHANNEL CONNECTIVITY, REALIZATION 2, SQ100-25 SCENARIO.	304
FIGURE 6.35. PRODUCTION AND INJECTION PROFILES FOR REALIZATION 6, SQ100-25 SCENARIO.....	305
FIGURE 6.36. CHANNEL PROXIMITY TO WELLS. REALIZATION 6, SQ100-25 SCENARIO.....	306
FIGURE 6.37. TOTAL FIELD PRODUCTION, 100-50 SCENARIO.....	307
FIGURE 6.38. PRODUCTION PROFILES OF SQ100-50 SCENARIO, REALIZATION 8.	308
FIGURE 6.39. CHANNEL PROXIMITY TO WELLS. SQ100-50 SCENARIO, REALIZATION 8.....	309
FIGURE 6.40. OIL SATURATION AT THE END OF 20 YEARS OF PRODUCTION, SQ100-50 SCENARIO, REALIZATION 2.	310
FIGURE 6.41. TOTAL FIELD PRODUCTION, 280-25 SCENARIO.....	311
FIGURE 6.42. CHANNEL PROXIMITY TO WELLS. SQ280-25 SCENARIO, REALIZATION 10.....	312
FIGURE 6.43. A COMPARISON OF THE SIMULATION RESULTS FOR THE COAST SCENARIO FOR ALL GRIDS.....	313
FIGURE 6.44. COMPARISON OF THE SIMULATION RESULTS OF THE BEACH SCENARIOS FOR THE SQUARE AND SDA GRIDS.	314
FIGURE 6.45. ULTIMATE PRODUCTION. SQUARE GRID, COAST SCENARIO.	315
FIGURE 6.46. RELATIVE CONTRIBUTION OF WELLS TO TOTAL FIELD PRODUCTION - BEACH SCENARIO, SQUARE GRID.....	316
FIGURE 6.47. OIL SATURATION AFTER 20 YEARS OF PRODUCTION - BEACH SCENARIO, SQUARE GRID - REALIZATION 2.....	317
FIGURE 6.48. TOTAL FIELD OIL PRODUCTION, 3-LAYER GRIDS OF THE COAST SCENARIO - REALIZATIONS 1–10.	318
FIGURE 6.49. SQUARE GRID, COAST SCENARIO.	319
FIGURE 6.50. FACIES MODEL OF COAST SCENARIO, SQUARE GRID, REALIZATION 1.	320
FIGURE 6.51. COAST SCENARIO, SQ500 x 400 x 3 GRID, REALIZATION 1.....	321
FIGURE 6.52. COAST SCENARIO, SQ500 x 400 x 3 GRID, REALIZATION 3.....	322
FIGURE 6.53 ULTIMATE PRODUCTION OR INJECTION FOR SQUARE GRID COAST SCENARIO.	323
FIGURE 6.54. ULTIMATE OIL PRODUCTION FOR LOWER ROUNDHEAD MEMBER SCENARIO.....	324
FIGURE 6.55. ULTIMATE OIL PRODUCTION BY WELL FOR THE LOWER ROUNDHEAD SCENARIO, 3-LAYER GRID DESIGNS.....	325
FIGURE 6.56. BASE MAP SHOWING THE ACTUAL FLOUNDER FIELD WELLS AND THE CONCEPTUAL VERTICAL WELLS (RED) USED FOR RESERVOIR SIMULATION.	326
FIGURE 6.57. FACIES MODEL OF THE LOWER ROUNDHEAD MEMBER AROUND WELL B. REALIZATION 3, LAYER 3.	327
FIGURE 6.58. POROSITY MODEL, LOWER ROUNDHEAD MEMBER MODEL. REALIZATION 3, LAYER 3—DETAIL AROUND WELL B.	328
FIGURE 6.59. CORRELATION COEFFICIENT (R) OF BASE GRID PRODUCTION AND UPSCALED GRID PRODUCTION VERSUS CELL-WIDTH TO SANDBODY-WIDTH RATIO (CSWR).	329

FIGURE 6.60. A COMPARISON OF THE RELATIONSHIP BETWEEN CORRELATION COEFFICIENT AND CSWR FOR THE SCENARIOS MODELLED.	330
FIGURE 6.61. %CHANGE VS. CSWR FOR ALL SCENARIOS.	331
FIGURE 6.63. REALIZATION 9, SQ100-25 SCENARIO. NO INJECTION.	333
FIGURE 6.65. COAST SCENARIO POROSITY GRIDS - REALIZATION 6, SQUARE GRID.	335
FIGURE 6.66. DETAIL OF MODELS AND WATER INJECTION PATHWAYS—REALIZATION 6, LAYER 2. 500 x 400 x 3 GRID.	336
FIGURE 6.67. WATER SATURATION AT 20 YEARS, LAYER 2 OF COAST MODEL, REALIZATION 6.	337
FIGURE 6.68. DETAIL OF MODELS AND WATER INJECTION PATHWAYS—REALIZATION 6, LAYER 2. 200 x 160 x 3 GRID.	338
FIGURE 7.1. NOMOGRAM FOR ESTIMATING THE POTENTIAL NUMBER OF CELLS IN A 3D MODEL.	355
FIGURE 7.2. CHART FOR ESTIMATING THE %CHANGE IN ULTIMATE PRODUCTION OF AN UPSCALED GRID.	356
FIGURE 7.3. MODEL OF THE UPPER VOLADOR FORMATION BARRIER-ISLAND SYSTEM.	357
FIGURE 7.4. OIL SATURATION AT THE END OF 20 YEARS PRODUCTION. SQ280-25, R7, LAYER 3.	358
FIGURE 7.5. COAST SCENARIO, SQUARE MODE, R5 LAYER 3.	359
FIGURE 7.6. CHANNEL PROXIMITY TO WELLS AND POROSITY DISTRIBUTION. SQ 100-25, REALIZATION 2.	360
FIGURE 7.7. CHANGE IN AVERAGE PORE VOLUME BY FACIES DISTRIBUTION COMPARED TO CHANNEL WIDTH AND POROSITY DISTRIBUTION. 100 M CHANNEL SCENARIOS.	361
FIGURE 7.8. CHANGE IN AVERAGE PORE VOLUME BY FACIES DISTRIBUTION COMPARED TO CHANNEL WIDTH AND POROSITY DISTRIBUTION. 280 M CHANNEL SCENARIOS.	362
FIGURE 7.9. AVERAGE FIELD PRODUCTION—ALL CHANNEL SCENARIOS.	363
FIGURE 7.10. AVERAGE %CHANGE IN FIELD PRODUCTION RELATIVE TO BASE GRID BETWEEN UPSCALED GRIDS AND THE BASE GRID FOR ALL CHANNEL SCENARIOS.	364
APPENDIX 1.1. CORE LOG, FLOUNDER 6ST1. TYPE WELL FOR THIS STUDY.	395
APPENDIX 1.2. CORE LOG, FLOUNDER A4.	396
APPENDIX 1.3. CORE LOG, FLOUNDER A2.	397
APPENDIX 1.4. CORE LOG, FLOUNDER 2.	398
APPENDIX 1.5. CORE LOG, FLOUNDER 3.	399
APPENDIX 2.1. VU.1 LOG SIGNATURE PLOT AND PALAEOFACIES MAP.	403
APPENDIX 2.2. VU.2 LOG SIGNATURE PLOT AND PALAEOFACIES MAP.	404
APPENDIX 2.3. VU.3 LOG SIGNATURE PLOT AND PALAEOFACIES MAP.	405
APPENDIX 2.4. VU.5 LOG SIGNATURE PLOT AND PALAEOFACIES MAP.	406
APPENDIX 2.5. RL.1 LOG SIGNATURE PLOT AND PALAEOFACIES MAP.	407
APPENDIX 2.6. RL.2 LOG SIGNATURE PLOT AND PALAEOFACIES MAP.	408
APPENDIX 2.7 RL.3 LOG SIGNATURE PLOT AND PALAEOFACIES MAP.	409
APPENDIX 2.8. RL.4 LOG SIGNATURE PLOT AND PALAEOFACIES MAP.	410
APPENDIX 2.9. RL.5 LOG SIGNATURE PLOT AND PALAEOFACIES MAP.	411
APPENDIX 2.10. RL.6 LOG SIGNATURE PLOT AND PALAEOFACIES MAP.	412
APPENDIX 2.11. RL.7 LOG SIGNATURE PLOT AND PALAEOFACIES MAP.	413
APPENDIX 2.12. RL.8 LOG SIGNATURE PLOT AND PALAEOFACIES MAP.	414
APPENDIX 2.13. RL.9 LOG SIGNATURE PLOT AND PALAEOFACIES MAP.	415
APPENDIX 2.14. RU.1 LOG SIGNATURE PLOT AND PALAEOFACIES MAP.	416
APPENDIX 2.15. RU.2 LOG SIGNATURE PLOT AND PALAEOFACIES MAP.	417
APPENDIX 2.16. RU.3 LOG SIGNATURE PLOT AND PALAEOFACIES MAP.	418
APPENDIX 2.17. RU.4 ESTUARY LOG SIGNATURE PLOT AND PALAEOFACIES MAP.	419
APPENDIX 2.18. RU.4 TRANSGRESSIVE LAG LOG SIGNATURE PLOT AND PALAEOFACIES MAP.	420
APPENDIX 3.1. HISTOGRAM OF POROSITY VALUES FOR THE 24 LAYER SDA100-25 SCENARIO.	423
APPENDIX 3.2. HISTOGRAM OF POROSITY VALUES FOR SSA100-25 SCENARIO.	424
FIGURE 3.3. POROSITY DISTRIBUTION OF SQ280-25 SCENARIO, 24 LAYERS.	425
FIGURE 3.4. POROSITY DISTRIBUTION, SQ280-50 SCENARIO, 24 LAYERS.	426
APPENDIX 3.5 POROSITY DISTRIBUTION OF SDA 280-25 SCENARIO, 24 LAYERS.	427
APPENDIX 3.6. POROSITY DISTRIBUTION OF SSA280-25 SCENARIO, 24 LAYERS.	428

APPENDIX 3.7. POROSITY DISTRIBUTION OF SQ 280-50 SCENARIO, 24 LAYERS. 429

APPENDIX 4.1. PORE VOLUME BY FACIES. 100-25 SCENARIO- ALL GRID DESIGNS. REALIZATIONS 1-3. 433

APPENDIX 4.2. PORE VOLUME BY FACIES. 100-50 SCENARIO- ALL GRID DESIGNS. 434

APPENDIX 4.3. COAST SCENARIO. A COMPARISON OF GRID DESIGNS AND THE CHANGES TO THE AVERAGE PORE VOLUMES ASSOCIATED WITH FACIES CAUSED BY VERTICAL AND HORIZONTAL UPSCALING. 435

APPENDIX 5.1. VERTICAL AND HORIZONTAL UPSCALING OF THE 100-25 SCENARIO, ALL GRID DESIGNS. 439

APPENDIX 5.2. VERTICAL AND HORIZONTAL UPSCALING OF THE 100-50 SCENARIO, ALL GRID DESIGNS. 440

APPENDIX 5.3. VERTICAL AND HORIZONTAL UPSCALING OF THE 280-25 SCENARIO, ALL GRID DESIGNS 441

APPENDIX 5.4. VERTICAL AND HORIZONTAL UPSCALING OF THE 280-50 SCENARIO, ALL GRID DESIGNS. 442

APPENDIX 5.5 VERTICAL AND HORIZONTAL UPSCALING OF THE 443

Table of Tables

TABLE 2.1. DETAILS OF THE CORES IN THE ZONE OF INTEREST.	16
TABLE 2.2. CORES INTERPRETED FOR THIS STUDY.	18
TABLE 2.3. FACIES ASSOCIATIONS AND THEIR DEPOSITIONAL ENVIRONMENTS.	28
TABLE 2.4. SYSTEMS TRACTS IN THE FLOUNDER FIELD.....	36
TABLE 6.1. GRID DESIGN AND CELL DIMENSIONS AND THEIR RELATIONSHIP TO CHANNEL WIDTHS.	265
TABLE 6.2. GRID DESIGN AND CELL DIMENSIONS AND THEIR RELATIONSHIP TO CHANNEL WIDTHS.	265
TABLE 6.3. CONTRIBUTION OF WELLS TO TOTAL FIELD PRODUCTION. SQUARE GRID, 100-25, 3 LAYERS.	267
TABLE 6.4. BREAKDOWN OF INDIVIDUAL WELL CONTRIBUTION TO TOTAL FIELD PRODUCTION—SQUARE GRID, COAST SCENARIO, 3 LAYERS.	269
TABLE 6.5. COAST SCENARIO—A COMPARISON OF THE RELATIVE CHANGE IN FIELD PRODUCTION BETWEEN A GRID AND ITS PRECEDING ONE.	270
TABLE 7.1. THE POINT AT WHICH POROSITY DISTRIBUTION BECOMES NORMAL FOR EACH CHANNEL WIDTH AND GRID DESIGN.	353

